Journal of Engineering Science and Technology
Vol. 17, No. 5 (2022) 3378 - 3392


# EVALUATION OF RADAR DOPPLER SIGNAL TIME-DOMAIN FEATURES FOR HAND GESTURE CLASSIFICATION

KHAIRUL KHAIZI MOHD SHARIFF[1,*], NOOR HAFIZAH ABDUL AZIZ[2], SAFIAH ZULKIFLI[3], MOHD MUSTAFA AWANG KECHIK[4]

[1]Microwave Research Institute, Universiti Teknologi MARA, Shah Alam, Malaysia
[2]School of Electrical Engineering, College of Engineering, Universiti Teknologi MARA, 40450 Shah Alam, Selangor, Malaysia
[3]School of Aerospace Engineering, Universiti Sains Malaysia, Pulau Pinang, Malaysia
[4]Department of Physics, Faculty of Science, Universiti Putra Malaysia, Selangor. Malaysia
*Corresponding Author: khairulkhaizi@uitm.edu.my

## Abstract

Hand gesture detection using Doppler radar has recently achieved great success. Typically, machine learning methods are used to separate the different hand gestures by feeding them with Doppler shift signals generated by the moving hands. While the success of machine learning-based classification of hand gestures has been primarily based on the use of spectral features, time-domain features-based recognition has received less attention so far. In this work, a set of time-domain features of Doppler signal is investigated in terms of their ability to separate hand gestures from a single subject performing four-hand gestures with a Doppler radar. The current study aims to investigate the potential of each time-domain features potential in recognising hand gestures. Using common machine-learning techniques, we presented the most stable single feature and multiset feature. The results show that zero-crossing (ZC) outperforms other features in all classification tests. The average classification accuracy for ZC was 80% and multiset features with ZC increase to 90%. The obtained result shows the capability of time-domain features, despite the simplicity of the method.

Keywords: Accuracy, Feature extraction, Radar sensor, Supervised machine learning, Time-domain features.

## 1. Introduction

Hand gesture is an unspoken body language that plays an important role in daily communications. Recently, hand-gesture recognition systems have become increasingly popular because of their potential applications in the area of human-computer interfaces (HCI) such as multimedia and game controls [1]. These interfaces seem to have several advantages when compared with the conventional keyboard. Firstly, hand gesture uses lower cognitive level than a keyboard, thus allowing more focus on the actual task. Secondly, they can be designed to work with natural actions of hand, which provide more intuitive and simple interaction with computer [2]. And thirdly, a hand gesture recognition system can be contactless, which enables ones to interact with a computer without endangering human life. For instance, to interact with the car multimedia devices and in the surgical room where the use of contactless hand gestures can eliminate the risk of cross-contamination [3, 4].

The two most commons approach in hand gesture detection are based on the use of a camera (RGB camera [5], and depth camera [6]), and wearable sensors (acceleration sensors [7] and electromyography [8]). While these approaches have shown to achieve a high rate of recognition accuracy, they suffer from several limitations. For the camera system, the accuracy is limited when operating in a noisy environment, such as in low lighting and bad weather conditions. Furthermore, it also raises concerns about the privacy of the users. On the other hand, the use of wearable sensors requires attaching several sensors on hand, which is deemed cumbersome and may limit the hand movements.

Alternatively, radar can solve the limitations in camera and wearable sensors. Radar preserves the anonymity of its use since it works by radiating low-power electromagnetic waves to hand, which then reflected to radar for measurement. Moreover, its operation is insensitive to dark surroundings and bad weather conditions. The recent development of low-cost and miniaturised Doppler radar is a promising technology to explore and to develop low-cost yet robust hand gesture recognition systems [9].

Hand gesture recognition is an intelligent signal processing technology that uses a classification algorithm to recognise the intent of the user. A typical classification algorithm extracts several features from the acquired signal and then used it to recognise the user hand gesture. The recognition is comprised of two processes: training and testing. During the training process, the classification algorithm "learns" the hand gesture based on the signal features presented to them. Subsequently, the testing is to validate how accurate the classification algorithm recognises the intended hand gesture.

Selecting "good" set of features which can effectively identify hand gestures is still an open challenge. In literature, the time-frequency domain (TFD) has been the primary source of features as the time-frequency signal consists of intricate Doppler components induced by the hand motions. Typically, TFD are generated using the efficient fast Fourier transform (FFT) algorithm. Although TFD features have been shown to provide high classification accuracy and robust [10-13], the FFT processing complexity can become very high with growing data samples because FFT involves $O(N\log_2 N)$ multiplications, where $N$ is the number of data samples [14]. For this reasons, recognition based on time-domain (TD) features is a promising approach for low-cost and real-time hand gesture recognition systems,

as this approach eliminates many complex signals processing such as signal transformation. Previous work has evaluated few TD features. These include zero-crossing and magnitude difference [15-16]. The results demonstrated that the TD features can achieve classification accuracy greater than 80%. While there are many TD features available in the literature, only two TD features have been investigated for radar applications. So far, there is no consensus yet on which TD features to suit the recognition task the best.

In this paper, we aim to 1) evaluate the performance of 8 common TD features using 4 classification algorithms and identify the TD features that provide the best accuracy. 2) evaluate the performance of the TD feature in a combined form or feature set.

Ideally, the outcome of this study could improve the design of more low-cost recognition systems for hand gestures based on radar and provide an alternative to the conventional TFD approach. Following this introductory part, Section II describes the methodology of the evaluation. Section III presents the evaluation results of the TD features, and finally, Section IV gives the concluding remarks.

## 2. Methodology

### 2.1. Radar time-domain signal acquisition

The time-domain Doppler signal used in this work was captured using a commercially available off-the-shelf Doppler radar named RFbeam K-LC2. The radar operates at a frequency of 24 GHz and produces in-phase (I) and quadrature (Q) outputs. The radar has a 4-patch antenna with an asymmetrical radiation beam of 34°/82° on vertical and horizontal and is suitable for short-range sensing applications [17].

The radar is connected to an intermediate board named RFbeam ST-100. This board consists of 73 dB two-stage and dual-channel low-noise amplifiers to amplify the I/Q signal from the radar. Subsequently, the analogue I/Q signal is digitised using a 16-bit onboard analogue to a digital converter (ADC). The data is sampled based on the standard digital audio rate of 44.1 kHz and transmitted to a computer by a standard universal serial bus (USB) [18].

The data collection setup was made simple following the goal of a practical and low-cost system. Figure 1 illustrates the general setup. The Doppler radar system was placed on 1.3 meters height table and facing the subject hand. The distance between the radar and the subject's palm was kept between 20- and 30-centimeters. The subject was a 23-year-old male and was standing during the data collection process. The environment was kept still from unwanted moving objects, for example, moving legs which can be presented as an unwanted Doppler signal.

Figure 2 depicts the morphology of the individual hand gestures involved in the experiment. The red line next to the hand indicates the gesture motions from start to finish. A total of four hand gestures are considered. These gestures are based on general movement applied to the fingers, palm, wrist, and forearm. The movement of each hand gesture also does not focus on a single finger or wrist gesture but consisting of motions that use multiple hand parts simultaneously. We named the gesture in Figure 2(a) to (d) as HG1, HG2, HG3, and HG4, respectively.

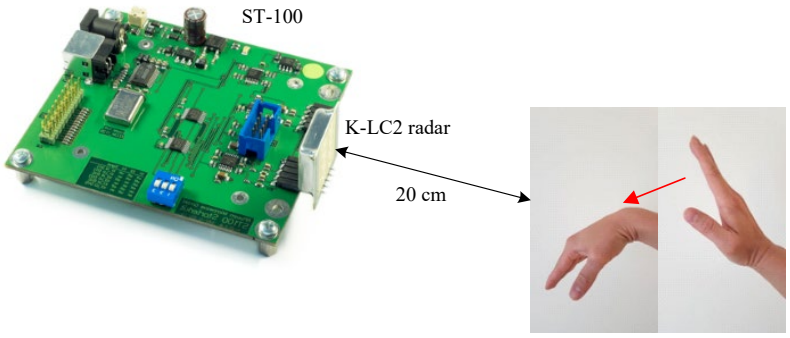


**Fig. 1. The main experimental setup: the K-LC2 radar, the ST-100 board, and hand gesture.**

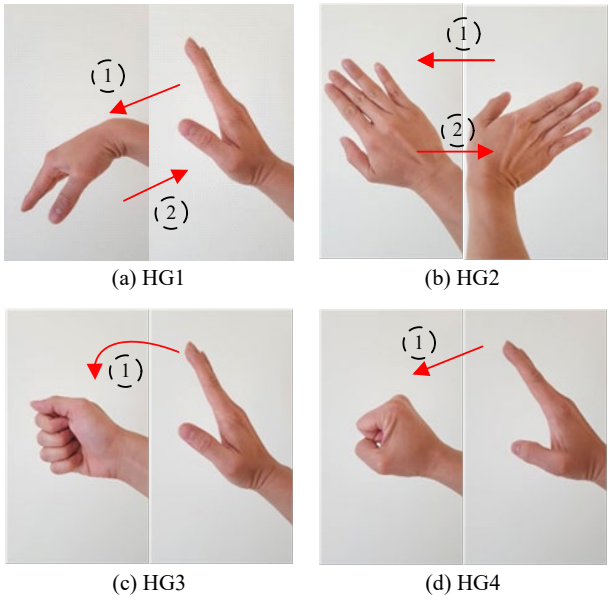


**Fig. 2. Estimated motions of each hand gesture: (a) swiping from top to down and back to top again, (b) swiping hand from right to left and to the right again, (c) clenching hand with 90 degrees rotation, and (d) clenching hand.**

A single trial was performed by executing each gesture one after another until the fourth gesture was completed. The same trials were repeated 75 times, accumulating 300 samples for each gesture and a total of 1200 samples for all hand gestures. It should be noted that within a trial, the subject keeps about two seconds delay between consecutive hand gestures. this delay is introduced to allow automatic segmentation of the signal in the next processing stage.

The hand gestures are recorded directly in a computer in the form of lossless audio format (.wav). Using an in-house MATLAB program, the audio files were transformed to MATLAB formatted file (.mat) and split the single audio signal into four separate segments containing individual hand gesture signals. A total of 1200

segments of Doppler are recorded in a matrix consisting of columns representing types of hand gestures and rows indicating the trial repetition.

An example of the Doppler signal for each hand gesture is shown in Fig. 3.

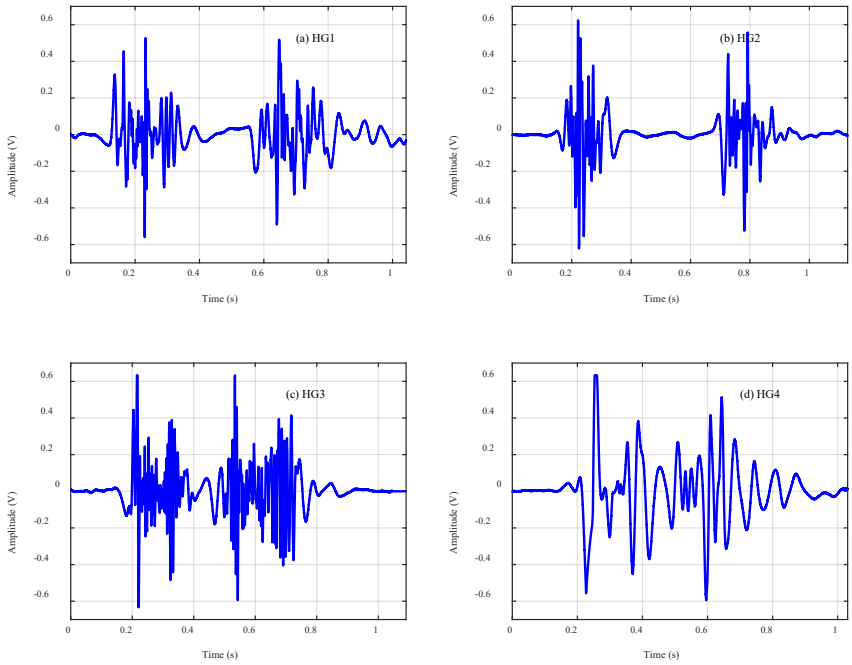


**Fig. 3. Example of time-series Doppler signal of each of the hand gestures.**

## 2.2. Signal filtering and amplitude normalisation

Filtering was performed to ensure that the extraction of TD features is robust against unwanted noises in the Doppler signal. Filtering is required for three main reasons. Firstly, the recording equipment, including the signal amplification in the ST100 board is not perfect thus, it may introduce a DC component on the waveform. This bias is removed using the following function [19]:

$$x'(n) = x(n) - \frac{1}{n}\sum_{n=0}^{N} x(n) \quad (1)$$

where $x(n)$ is the Doppler signal and $x'(n)$ is the Doppler signal with no DC offset. Secondly, high frequency "flicker" introduced by the surrounding environment may exist on the waveform. This noise appears on the waveform as local maxima or minima which may distort the true shape of the signal. We eliminated this noise using a 1 kHz third-order Butterworth Low Pass Filter (LPF). Most of the Doppler signal power resides in the frequency range between 10 to 600 Hz thus, the cut-off frequency at 1 kHz is considered suitable. Thirdly, it is difficult to guarantee the gesturing distance between hand and radar is kept perfectly between 20- and 30-centimeters during the duration of the data collection process. Gesturing at significantly different lengths (>20 centimetres) causes amplitude variance between the same type of hand gesture. Our attempt to reduce the variance was normalised with zero mean and unit variance across the repetitions data.

## 2.3. Time-domain features

Various TD features have been investigated in the past for recognition problems such as in machine fault classification [20], brain-computer communications [21], and epileptic signal classification [22]. The majority of these features are computationally inexpensive and efficient because they are measured straight from the waveform amplitudes and require no signal transformation.

In line with the theme of a low-cost hand gesture recognition system, we selected eight TD features found in the literature. This work aims to investigate the potentials of these TD features and highlight their potential. The following are the names: 1) mean absolute value, 2) variance, 3) root-mean-square, 4) logarithmic mean, 5) zero-crossing, 6) slope sign change, 7) temporal moment, and 8) waveform length. Subsequently, the following briefly defines each of these features.

**a) Absolute mean value**

Abbreviated *AMV*. This feature measures the absolute mean of signal *x* of a Doppler signal length *N*, and it is given by Phinyomark et al. [23]:

$$MVA = \frac{1}{N}\sum_{n=0}^{N} x(n) \tag{2}$$

**b) Variance**

Abbreviated *VAR*. This feature computes the Doppler signal's power, and it's given by [23]:

$$VAR = \frac{1}{N-1}\sum_{n=0}^{N} |x(n)|^2 \tag{3}$$

**c) Waveform length**

Abbreviated *WL*. This feature measures the cumulative length of the Doppler signal over the length *N*. WL is defined by [23]:

$$WL = \sum_{n=0}^{N} x(n+1) - x(n) \tag{4}$$

**d) Slope sign change**

Abbreviated *SSC*. This feature counts how many times the sign of slope in the Doppler changes its sign within window length *N*. Additionally, a threshold is employed in the SSC to minimise the effect of flicker noise on the Doppler signal. The SSC is defined by [23]:

$$SSC = \frac{1}{N}\sum_{n=0}^{N}\left[f[(x(n) - x(n-1)) \cdot (x(n) - x(n+1))]\right]$$

$$sgn(x) = \begin{cases} 1 & if x \geq Th2 \\ 0 & \text{otherwise} \end{cases} \tag{5}$$

where *Th*2 is the threshold. In this work, the threshold was 40 mV, equivalent to 3 standard deviations of flicker noise.

**e) Zero-crossing**

Abbreviated *ZC*. This feature finds the dominant frequency within a second. ZC is calculated by counting the number of sign changes of amplitude, either from positive amplitude to negative amplitude or vice versa. Additionally, to make the

measurement robust, a threshold condition is employed to remove low amplitude noise. The ZC is given by [23]:

$$ZC = \frac{1}{N}\sum_{n=0}^{N} sgn(x(n) \cdot x(n+1) \cap |x(n) \cdot x(n+1)| \geq Th1)$$
$$sgn(x) = \begin{cases} 1 & if x \geq Th1 \\ 0 & \text{otherwise} \end{cases} \quad (6)$$

where $Th1$ is the threshold. In this work, we used threshold = 60 mV.

**f) f) Root-mean-square**

Abbreviated *RMS*. This feature computes the magnitude of the AC waveform in the Doppler signal. It is defined by [23]:

$$RMS = \sqrt{\frac{1}{N}\sum_{n=0}^{N}|x(n)|^2} \quad (7)$$

**g) Temporal moment**

Abbreviated *TM*. This feature measures the characteristics shape of the Doppler signal. TM is defined by [23]:

$$TM = \frac{1}{N}\sum_{n=0}^{N} x^4(n) \quad (8)$$

Using the moment order, $M = 4$, we estimated the kurtosis of the Doppler signal.

**h) Logarithmic difference absolute mean value**

Abbreviated *LOG*. This feature calculates the logarithmic non-linear characteristics of the Doppler signal, which can be defined by Phinyomark et al. [24]:

$$LOG = log\left(\frac{1}{N}\sum_{n=0}^{N}|x(n+1) - x(n)|\right) \quad (9)$$

The features from (a) to (h) were extracted from the dataset, and their values were arranged into a single matrix. Successively, labels to the values were given according to their intent gesture to form a hand gesture dataset.

## 2.4. Classification and testing

Performing classification on the different hand gestures can be achieved either via supervised learning techniques or unsupervised learning techniques. In the supervised learning method, the algorithm is feed with teaching data, and on this basis, the algorithms generate a model according to the desired output. On the other hand, unsupervised machine learning works in the way that it does not need teaching data but rather finds statistical properties of the data that can be used to train the algorithm [25]. While the unsupervised learning techniques is less complex because data label is not needed, the algorithm requires a large amount of data.

We employed 4 common supervised machine learning algorithms to evaluate the quality of the features. They are 1) decision tree, 2) Naïve Bayes, 3) *k*-nearest neighbour (*k*NN), and 4) support vector machine (SVM). Accordingly, the configuration used related to each classifier is presented in Table 1.

**Table 1. The hyperparamters employed by each classifier.**

| Classifier | Configuration |
|---|---|
| **Decision Tree** | Algorithm: ID3 |
| **Naïve Bayes** | Distribution type: Gaussian |
| ***k*NN** | $k = 3$ |
| | Distance method: Euclidean |
| **SVM** | Kernel: Radial basis function (RBF) |

The portioning of the dataset for training and testing was prepared based on the $k$-fold cross-validation procedure. Since the dataset containing 1200 values is large, $k = 10$ was chosen. For $k = 10$, the dataset is portioned into 10 groups, of which 9 groups are used to train the classifiers, and one is used for testing. These data were fed to the classifiers, which learn the hand gestures patterns according to the labelled dataset.

Percentage accuracy was chosen as the performance metric to evaluate the ability of the TD features in combination with the classifier algorithm. The accuracy in recognising a type of hand gesture is given by:

$$Accuracy = \frac{\text{Noofcorrectclassification}}{\text{Totalclassifiednumber}} \times 100\% \quad (10)$$

Many studies in classification problems practice a combination of two or more features to increase classification accuracy. For this reason, we also investigated the capability of the features as a set of combined features.

All classification and testing were performed using MATLAB machine learning toolbox and some in-house built MATLAB programs on a portable computer with the following specifications: Intel i5-5300U 2.3 GHz CPU and 8 gigabytes of RAM.

## 3. Results

Figure 4 shows the comparison of classification accuracy of each TD feature in terms of different classifiers. The horizontal bars in the figure are sorted in ascending order according to their average classification accuracy. Apart from that, Table 2 presents the average classification accuracy of each feature as an indicator of their general ability.

Based on the results, the use of ZC yielded the highest classification accuracy (80%), followed by SSC (63%). Meanwhile, the use of RMS, VAR, MVA, and TM produced the poorest accuracy. The maximum standard deviation of the classification accuracy for all eight features was 12%. This measure indicates that the features show robust properties in the context that their accuracy does not change so much when tested with different classification algorithms.

Next, we evaluated the performance of the features in combination. We considered the top 50% of features in Table 2 to create a new set of multiple features. The new features were configurated as follows: 1) ZC + SSC, 2) ZC + SSC + WL, and 3) ZC + SSC + LOG. Their performance in classifying hand gestures is presented in Fig. 5. For comparison purposes, the performance of ZC, SSC, and all-eight-feature combined are also added in the same figure to compare

the accuracy from the smallest to the biggest feature. Additionally, Table 3 is presented to show the average accuracy as a function of feature combination.

Results show that the multiple features set increases the classification accuracy between 83% to 91% compared to the single features. The highest accuracy was achieved with all features combined. In the case of the lower number of feature combinations, the best feature is ZC + SSC + LOG because it provides the highest accuracy boost (11%) from the single feature ZC. Moreover, the multiple features show consistent performance between classifiers, indicating that they are stable.

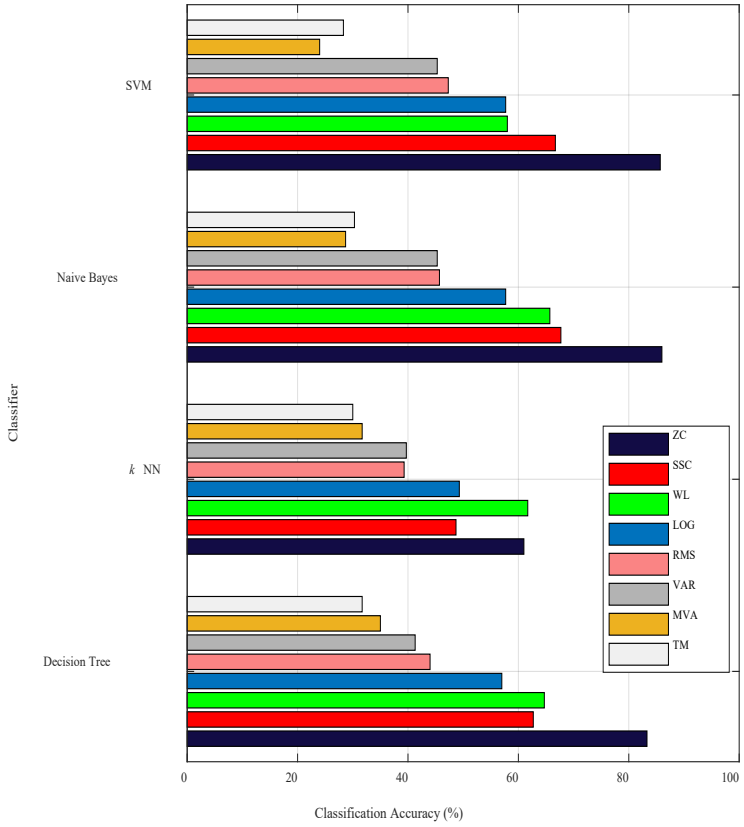


**Fig. 4. The comparison of classification accuracy using four types of classifiers with eight TD features.**

**Table 2. Average classification accuracy across 4 classifiers.**

| | TD feature | Avg. accuracy | | TD feature | Avg. accuracy |
|---|---|---|---|---|---|
| 1 | ZC | 80% | 5 | RMS | 44% |
| 2 | SSC | 63% | 6 | VAR | 42% |
| 3 | WL | 61% | 7 | MVA | 30% |
| 4 | LOG | 55% | 8 | TM | 29% |

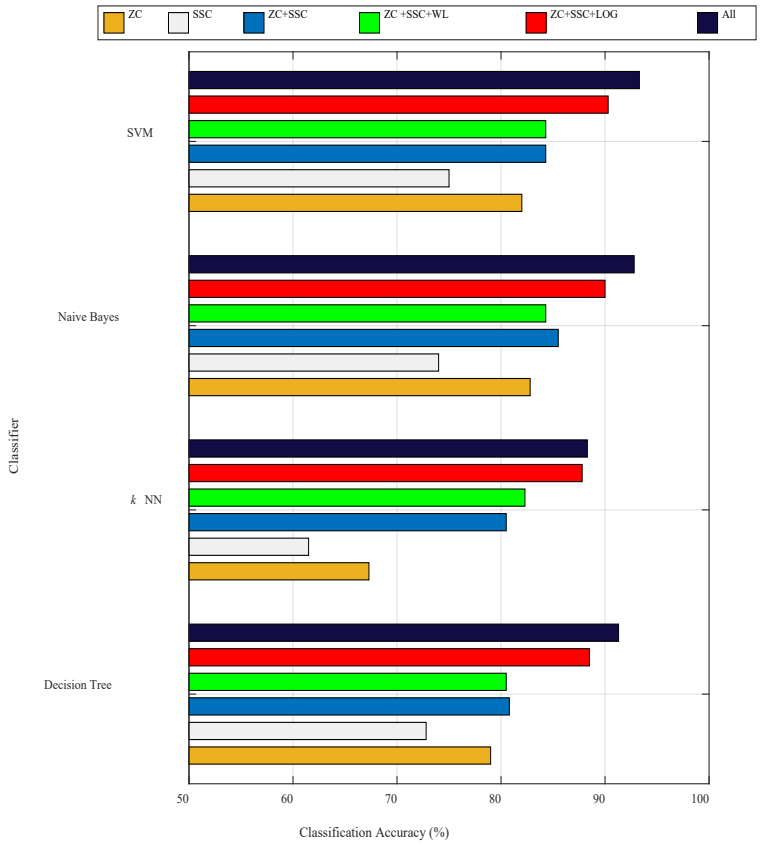


**Fig. 5. The comparison classification accuracy of four classifiers with six feature configurations.**

**Table 3. Average classification accuracy across 4 classifiers.**

| | TD feature | Average accuracy | | TD feature | Average accuracy |
|---|---|---|---|---|---|
| 1 | SSC | 63% | 4 | ZC + SSC + WL | 83% |
| 2 | ZC | 80% | 5 | ZC + SSC + LOG | 90% |
| 3 | ZC+ SSC | 83% | 6 | ALL | 91% |

Subsequently, we computed two confusion matrices to show the influence of feature selection on the inter-dependency among hand gestures classification accuracy. We arbitrarily choose naïve bayes as the classifier for this demonstration. Figure 6 shows two confusion matrices. In Fig 6(a), the classification is based on ZC + SSC, and in Fig 6(b) is based on ZC + SSC + LOG. The total data per hand gesture was set to 75 and the percentage instances in shown in each box. As can be seen from both confusion matrices, hand gestures show results near 100%. However, even employing multiple features set on the data, the error between classifying hand gesture 1 (HG1) and 4 (HG4) cannot be resolved easily. This is expected since both of the gesture is closely similar.

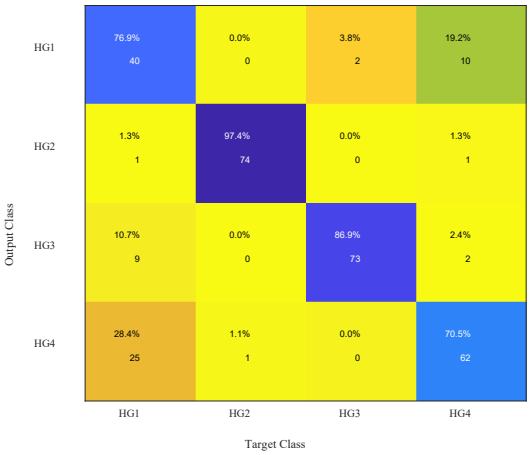


(a) ZC

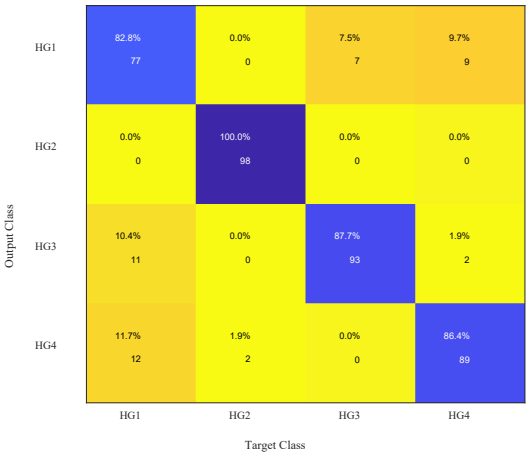


(b) ZC + SSC + LOG

**Fig. 6. Confusion matrix for classification based on (a) ZC and (b) ZC + SSC + LOG.**

## 4. Discussion

Practical use of time-domain features for radar-based hand gesture recognition systems requires that the features be insensitive to noise and the performance remains consistent across the usage period. Thus, these requirement raise the need to recognise the effects of the disturbances in typical hand gestures signal to the selected features.

Our work achieved the aim to analyse best eight TD feature which could inform designers in developing a low-cost and robust recognition system. We quantified the performance of the time-domain feature using actual hand gesture signals and test them on popular classifiers. Since the ability of the features is tested based on their classification accuracy, the outcome of this study may benefit the new design of the hand gesture recognition system by selecting the best time-domain features.

Compared to the work in [15-16] which evaluated time-domain features, the achieved level of accuracy here is lower between 10% to 20%. This may be due to the different types of gestures were used, different experimental setups, and different methods of validation. Nonetheless, all studies, including in this paper, indicate that ZC is a robust time-domain feature.

One of the obvious trends in our result is the performance of ZC and SSC features. Both features show higher accuracy and stability compared to MVA, RMS, and VAR. The probable reason for good accuracy for ZC and SSC is because these features are related to the frequency of the signal [26], on the other hand, the MVA, RMS, and VAR are estimates of magnitude properties of the signal. Our further investigation found that the magnitude variability of signals within the same hand gesture label was considerably large. It is worth noting that, a hand has a very small radar cross-section which directly affects the energy contours of Doppler signals [27].

To summarise in the context of actual implementation perspective, the proposed TD features are able to classify hand gesture signals with sufficiently high accuracy (80%). When feature set are adopted, a relatively higher classification accuracy can be obtained. Furthermore, higher computational efficiency can be obtained with longer data length.

## 5. Conclusions

In this paper, the use of time-domain features namely AMV, VAR, WL, SSC, ZC, RMS, LOG, and TM were investigated for hand gesture classification based on Doppler radar technology. The collected hand gesture signals were filtered and normalised before classification.

Next, the eight features were extracted from the conditioned signal, and then we formed a time-domain feature dataset. Four popular classifiers namely SVM, naïve bayes, kNN, and decision tree were used, and they are trained and validated according to the 10-fold cross-validation approach.

The examination was performed to determine the capability of each time-domain feature in classifying different hand gestures. In the first analysis, the features were evaluated as independent features and, in the second analysis, they are evaluated as a set of multiple feature combinations.

Results from both analyses showed the promising potential of time-domain-based features in hand gesture classification. We found that the zero-crossing features provide the highest accuracy, achieving 80% on their own and 90% in the multi-feature configuration (ZC + SSC + LOG). Accordingly, features related to frequency estimation show higher classification accuracy. The features also show stable performance with little variation across the analysis.

The findings in this paper can be used in the development of a low-cost hand gesture system based on Doppler radar.

For future work, we aimed to investigate hand gesture signals that are "orthogonal" to each other. For example, finding hand gesture signals that are so different between them, so that the classification accuracy can be further improved by using the time-domain features investigated here.

**Nomenclatures**

| | |
|---|---|
| $k$ | Neighbour value for the nearest neighbour algorithm |
| $n$ | The $n^{th}$ sample of Doppler signal |
| $TH1$ | A threshold value for noise removal in the ZC algorithm, V |
| $TH2$ | A threshold value for noise removal in SSC algorithm, V |
| $x$ | Discrete sample of time-domain Doppler signal, V |

**Abbreviations**

| | |
|---|---|
| ADC | Analogue to digital converter |
| AMV | Absolute mean value |
| CPU | Central processing unit |
| DC | Direct current |
| HCI | Human-computer interaction |
| HG | Hand gesture |
| I/Q | In phase and quadrature signal |
| *k*NN | k-nearest neighbour |
| LOG | Logarithmic difference absolute mean value |
| LPF | Low pass filter |
| RAM | Random-access memory |
| RGB | Red, green, and blue |
| RMS | Root mean square |
| SSC | Slope sign change |
| SVM | Support vector machine |
| TD | Time-domain |
| TFD | Time-frequency domain |
| TM | Temporal moment |
| USB | Universal serial bus |
| VAR | Variance |
| WL | Waveform length |
| ZC | Zero crossing |

## References

1. Liu, H.; and Wang, L., (2018). Gesture recognition for human-robot collaboration: A review. *International Journal of Industrial Ergonomics*, 68, 355-367.
2. Shanthakumar, V.A.; Peng, C.; Hansberger, J.; Cao, L.; Meacham, S.; and Blakely, V. (2020). Design and evaluation of a hand gesture recognition approach for real-time interactions. *Multimedia Tools Applications*, 79(25), 17707-17730.
3. D'Eusanio, A.; Simoni, A.; Pini, S.; Borghi, G.; Vezzani, R.; and Cucchiara, R. (2020). Multimodal hand gesture classification for the human-car interaction. *Informatics*, 7(3), 31.
4. Bockhacker, M.; Syrek, H.; Von Elster, M.E.; Schmitt, S.; and Roehl, H. (2020). Evaluating usability of a touchless image viewer in the operating room. *Applied Clinical Informatics*, 11(1), 88-94.
5. Oudah, M.; Al-Naji, A.; and Chahl, J. (2020). Hand gesture recognition based on computer vision: A review of techniques. *Journal of Imaging*, 6(8), 73.

6. Ren, Z.; Meng, J.; and Yuan, J. (2011). Depth camera based hand gesture recognition and its applications in human-computer-interaction. *Proceedings of* 2011 8*th International Conference on Information*, *Communications & Signal Processing*, Singapore, 1-5.
7. Zeng, Y.; Yang, Z.; Cao, W.; and Xia, C. (2010). Hand-motion patterns recognition based on mechanomyographic signal analysis. *Proceedings of* 2009 *International Conference on Future BioMedical Information Engineering* (*FBIE*), Sanya, China, 21-24.
8. Jaramillo-Yánez, A.; Benalcázar, M.E.; and Mena-Maldonado, E. (2020). Real-time hand gesture recognition using surface electromyography and machine learning: A systematic literature review. *Sensors*, 20(9), 2467.
9. Pauli, M.; Göttel, B.; Scherr, S.; Bhutani, A.; Ayhan, S.; Winkler, W.; and Zwick, T. (2017). Miniaturized millimeter-wave radar sensor for high-accuracy applications. *IEEE Transactions on Microwave Theory Technology*, 65(5), 1707-1715.
10. Lu, Y.; and Lang, Y. (2020). Sign language recognition with CW radar and machine learning. *Proceedings of* 2020 21*st International Radar Symposium* (*IRS*), Warsaw, Poland, 31-34.
11. Zhang, S.; Li, G.; Ritchie, M.; Fioranelli, F.; and Griffiths, H. (2016). Dynamic hand gesture classification based on radar micro-Doppler signatures. *Proceedings of the* 2016 *CIE International Conference on Radar* (*RADAR*), Guangzhou, China, 1-4.
12. Amin, M.G.; Zeng, Z.; and Shan, T. (2019). Hand gesture recognition based on radar micro-doppler signature envelopes. *Proceedings of* 2019 *IEEE Radar Conference* (*RadarConf*), Boston, USA, 1-6.
13. Sun, Y.; Fei, T.; Schliep, F.; and Pohl, N. (2018). Gesture classification with handcrafted micro-doppler features using a FMCW radar. *Proceedings of* 2018 *IEEE MTT-S International Conference on Microwaves for Intelligent Mobility* (*ICMIM*), Munich, Germany, 1-4.
14. Liu, S.; Shan, T.; Tao, R.; Zhang, Y.D.; Zhang, F.; and Wang, Y. (2014). Sparse discrete fractional fourier transform and its applications. *IEEE Transactions on Signal Processing*, 62(24), 6582-6595.
15. Miller, E.; Li, Z.; Mentis, H.; Park, A.; Zhu, T.; and Banerjee, N. (2020). RadSense: enabling one hand and no hands interaction for sterile manipulation of medical images using doppler radar. *Smart Health*, 15, 100089.
16. Wan, Q.; Li, Y.; Li, C.; and Pal, R. (2014). Gesture recognition for smart home applications using portable radar sensors. *Proceedings of* 2014 36*th Annual International Conference of the IEEE Engineering in Medicine and Biology Society*, Chicago IL, USA, 6414-6417.
17. RFbeam, (2020). Standard product K-LC2 dual channel radar transceiver. Retrived January 5, 2022, from https://www.rfbeam.ch/product?id=5.
18. RFbeam, (2020). Standard Product ST100 starter kit. Retrived January 5, 2022, from https://www.rfbeam.ch/product?id=34.
19. Zelinka, I.; Chen, G.; Rössler, O.E.; Snasel, V.; and Abraham, A. (2013). *Nostradamus* 2013*: Prediction*, *modeling and analysis of complex systems*. Springer Science & Business Media.

20. Jan, S.U.; Lee, Y.-D.; Shin, J.; and Koo, I. (2017). Sensor fault classification based on support vector machine and statistical time-domain features. *IEEE Access*, 5, 8682-8690.
21. Vidaurre, C.; Krämer, N.; Blankertz, B.; and Schlögl, A. (2009). Time domain parameters as a feature for EEG-based brain-computer interfaces. *Neural Networks*, 22(9), 1313-1319.
22. Fasil O.K.; and Rajesh. R. (2019). Time-domain exponential energy for epileptic EEG signal classification, *Neuroscience Letters*, 694, 1-8.
23. Phinyomark, A.; Phukpattaranont, P.; and Limsakul, C. (2012). Feature reduction and selection for EMG signal classification. *Expert System Applications*, 39(8), 7420-7431.
24. Phinyomark, A.; Quaine, F.; Charbonnier, S.; Serviere, C.; Tarpin-Bernard, F.; and Laurillau, Y. (2014). Feature extraction of the first difference of EMG time series for EMG pattern recognition. *Computer Methods and Programs in Biomedicine*, 117(2), 247-256.
25. Berry, M.W; Mohamed, A.; and Yap, B.W. (2019). *Supervised and unsupervised learning for data science*. Springer Nature.
26. Tkach, D.; Huang, H.; and Kuiken, T.A. (2010). Study of stability of time-domain features for electromyographic pattern recognition. *Journal of NeuroEngineering and Rehabilitation*, 7, 21.
27. Hügler, P.; Geiger, M.; and Waldschmidt, C. (2016). RCS measurements of a human hand for radar-based gesture recognition at E-band. *Proceedings of German Microwave Conference* (*GeMiC*), Bochum, Germany, 259-262.